Understanding linkages between global climate indices and terrestrial water storage changes over Africa using GRACE products

R.O. Anyah[a], E. Forootan[b,c], J.L. Awange[b], M. Khaki[b]

[a]*Dept. of Natural Resources and the Environment, University of Connecticut, USA*
[b]*School of Earth and Planetary Sciences, Discipline of Spatial Sciences, Curtin University, Perth, Australia.*
[c]*Geodetic Institute, Karlsruhe Institute of Technology, Karlsruhe, Germany*

Abstract

Africa, a continent endowed with huge water resources that sustain its agricultural activities is increasingly coming under threat from impacts of climate extremes (droughts and floods), which puts the very precious water resource into jeopardy. Understanding the relationship between climate variability and water storage over the continent, therefore, is paramount in order to inform future water management strategies. This study employs Gravity Recovery And Climate Experiment (GRACE) satellite products and the higher order (fourth order cumulant) statistical independent component analysis (ICA) method to study the relationship between Terrestrial Water Storage (TWS) changes and five global climate-teleconnection indices; El Niño-Southern Oscillation (ENSO), North Atlantic Oscillation (NAO), Madden-Julian Oscillation (MJO), Quasi-Biennial Oscillation (QBO) and the Indian Ocean Dipole (IOD) over Africa for the period 2003-2014. Pearson correlation analysis is applied to extract the connections between these climate indices (CIs) and TWS, from which some known strong CI-rainfall relationships (e.g., over equatorial eastern Africa) are found. Results indicate *unique linear-relationships* and *regions* that exhibit strong linkages between CIs and TWS. Moreover, unique regions having strong CI-TWS connections that are completely different from the typical ENSO-rainfall connections over eastern and southern Africa are also identified. Furthermore, the results indicate that the first dominant Independent Components (IC) of the CIs are linked to NAO, and are characterized by significant reductions of TWS over southern Africa. The second dominant ICs are associated with IOD and are characterized by significant increases in TWS over equatorial eastern Africa, while the combined ENSO and MJO are apparently linked to the third ICs, which are also associated with significant increase in TWS changes over both southern Africa as well as equatorial eastern Africa.

Keywords:
Africa, Terrestrial Water Storage (TWS), Climate Indices, GRACE, ENSO, IOD, NAO, MJO, QBO, Climate-TWS Hotspots

1.0 Introduction

Africa, the world's poorest continent faces myriad of climate-related extremes, e.g., droughts and floods (see, e.g., Lyon et al., 2014, Omondi et al., 2014, Awange et al., 2016a, Mpelesoka et al., 2017, Ndehedehe et al., 2018), which fuel food insecurity thereby putting millions of lives at risk (e.g., Agutu et al., 2017). Given the large dependency of the continent on rain-fed agriculture

(Agola and Awange 2015, Agutu et al., 2017), understanding the relationship that exists between Terrestrial Water Storage (TWS; i.e., a summation of soil moisture, groundwater, surface, and vegetation water storage compartments) and global climate teleconnection indices is essential for agricultural production on the one hand, and for improving the understanding of interactions between climate variability (through, e.g., climate indices) and the water cycle on the other hand. This is also important for managing the water resources in arid and semi-arid regions of the continent, and for the general planning purposes in order to make the continent food secure. Whereas the relationships between climate indices and rainfall is relevant for meteorological drought mitigation (e.g., Clark et al., 2003, Naumann et al., 2014, Kurnik et al., 2011, Awange et al., 2016a, 2016b, and Mpelesoka et al., 2017), it is also vital to understand the relationship between climate indices and TWS in order to be able to mitigate both hydrological drought as well as agricultural droughts (e.g., Anderson et al., 2012; AghaKouchak, 2015).

Although a number of studies have previously investigated and discussed the relationships between global climate indices and rainfall over the African continent (e.g., Becker et al., 2010; Indeje et al., 2000; Mutai and Ward 2001; Awange et al., 2013), the relationship between some of the dominant global climate teleconnection indices and seasonal/inter-annual variability of TWS has not been extensively investigated, except a few recent studies such as Reager and Famiglieti, (2009), Phillips et al., (2012), Awange et al., (2013), Forootan et al., (2014a) and Ndehedehe et al., (2017a, 2018). However, these studies also focus on separate sub-regions of the continent and thus do not consider the entire continent to provide a more comprehensive understanding of the relationship between the continent's TWS and major global climate teleconnection indices. For instance, Awange et al. (2013) look at the Lake Victoria basin in East Africa while Forootan et al., (2014a) and Ndehedehe et al., (2017a, 2018) consider the West Africa region. The reason for this is largely due to the fact that a comprehensive measurement of the components of TWS (surface water, groundwater, soil moisture, snow/ice and biomass) from the insufficient and unreliable in-situ hydroclimate data remains a big challenge (e.g., Creutzfeldt et al., 2010). TWS comprises all forms of water stored on the surface and in the subsurface of the Earth, which is a major component of the hydrological cycle and is critical in understanding the land surface-atmosphere interactions, and exchanges of moisture and energy.

Since 2002, however, large-scale TWS has been successfully estimated using the gravity observations of Gravity Recovery And Climate Experiment (GRACE, e.g., Tapley et al., 2004). Nominal monthly GRACE TWS can be derived with an accuracy of ~1 cm with few hundred km spatial resolution. GRACE has been applied globally to study the relationship between climate variability and TWS changes. For example, Phillips et al., (2012) and Ni et al., (2018) examined linkages between ENSO and global TWS over the entire globe. Using monthly GRACE-TWS for the period 2003-2010, Phillips et al., (2012) showed peak correlations between Multivariate ENSO Index (MEI) and the measured (GRACE) mass anomaly time series to be fairly high for the Amazon Basin and Borneo in Southeast Asia. However, other tropical regions showed strong negative correlations with MEI, while arid regions indicated high positive correlations. Phillips et al., (2012) concluded that using GRACE satellite data and ENSO index helped to isolate teleconnection patterns around the globe, showing areas where ENSO and TWS were highly correlated. Other studies that have employed GRACE to study climate-related impacts include Chen et al., (2010), Becker et al., (2010), Thomas et al., (2014), Zhang et al., (2015), Cao et al., (2015) and Kushe et al., (2016). Given ENSO's dominant impact on global TWS changes,

statistical decomposition techniques are developed and applied in Eicker et al. (2016) and Forootan et al. (2018) to separate variations in TWS that are related to ENSO from the rest, which are called 'non-ENSO' modes. Such separation seems to be significant to understand TWS trends without the impact of extreme events such as those associated with ENSO. These studies, however, are global in nature and those that consider various parts of the African continent do not explore the impact of other major climate indices such as Madden-Julian Oscillation (MJO), and Quasi-Biennial Oscillation (QBO) on TWS changes at continental scale. For instance, Forootan et al, (2014a) showed that there is significant influence of NAO and ENSO on annual and inter-annual variability of TWS over West Africa while Ndehedehe et al., (2017) examined the association of three global climate indices (ENSO, IOD, and Atlantic Multi-decadal Oscillation AMO) with changes in TWS derived from both Modern-Era Retrospective Analysis for Research and Applications (MERRA, 1980–2015) and Gravity Recovery and Climate Experiment (GRACE, 2002–2014). The present contribution aims at filling this gap by not only considering ENSO, IOD, and NAO that have been treated in parts of Africa as discussed above, but also two additional climate indices (i.e., MJO and QBO), which have not previously been considered, and are also known to influence seasonal and intra-seasonal rainfall variability over parts of Africa (e.g. Semazzi and Indeje, 1999). For the first time, a study of the linkages between these five major climate indices and TWS is undertaken over the entire continent of Africa, known to be in-situ data deficient. This pioneering continent-wide study of climate variability impacts on the stored water of the continent will provide useful information for some areas that have hardly been covered.

Therefore, the present study specifically contributes the following; (i) it provides an analysis of possible linear and non-linear relationships between five common global climate indices (NAO, QBO, ENSO, IOD, MJO) and GRACE-derived TWS data (hereafter referred to simply as GRACE-TWS) over the entire African continent, (ii), it provides an analysis of both phase-locked and lagged correlations between these key global climate indices and TWS changes at sub-seasonal, annual, and decadal time scales, and (iii), it applies a higher order statistical method of Independent Component Analysis (ICA, Forootan and Kusche, 2012, 2013) to filter the interrelationships among the five global climate indices and isolate any unique or combined influences of these indices on TWS changes of the African continent. This enables identification of unique regions where such relationships are strongest, which is important for water resources assessments and management.

The rest of this study is organized as follows; in section 2, the study domain is presented, while section 3 briefly describes the five global climate indices that have been correlated with TWS data in this study. Section 4 analyses and discusses the results Section 5 provides the major conclusions of the study.

2.0 Study Domain

The relationships between the global climate teleconnection indices and TWS over Africa (Figure 1) can be understood within the context of the general climatology since the drivers of climatological-rainfall patterns over the continent also influence terrestrial water storage recharge in the soil, surface and groundwater bodies. The drivers of the general climate (hydroclimate) of Africa are dominated by atmospheric circulation systems (e.g., monsoonal trade winds) and land surface processes, which influence inter-tropical convergence zone

(ITCZ), where these winds (and rain-generating moisture) normally converge and affect rainfall patterns. The ITCZ over the African continent has a north-south migration pattern dictated by the position of the overhead sun and tend to influence the location of maximum precipitation, with approximately 3-4 weeks lag time (see e.g., Nicholson, 1996).

Seasonal rainfall distribution over areas south of the Sahara is particularly linked to the movement and position of the ITCZ. However, over the equatorial regions, rainfall tends to be evenly distributed throughout the year (i.e., showing limited dependence on the ITCZ). For higher latitudes, however, especially over the Sahel, rainfall tends to be confined to the summer months-June-September (e.g., Ndehedehe et al., 2016). Over equatorial eastern Africa, rainfall tends to be highly influenced and dictated by southeast and northeast monsoons, depending on the north-south migration of the ITCZ position. Southern African rainfall, on the other hand, tends to exhibit spatio-temporal rainfall distribution largely influenced by major circulation features of the southern hemisphere. For example, from the equator to about 20^{o}S, seasonal rainfall variability tend to be in synch with the movement of the ITCZ whereas the more sub-tropical regions are influenced by semi-permanent high-pressure cells of the general circulation of the atmosphere, characterized by a high degree of intra- and inter-annual variability (Tyson, 1986).

In general, as a whole, apparent linkages exist between the global climate indices and rainfall, and to an extent with TWS over a number of regions in sub-Saharan Africa (see, e.g., Ndehedehe et. al., 2017a, 2018). It is important to note, however, that there may be several other human-induced factors that may contribute to TWS patterns and changes – factors that have not been explicitly factored into our computations and analysis. For example, at the local scale, the effects of complex terrain (topography) and large inland water bodies could be superimposed on the climatological patterns, leading to unique space-time distribution of rainfall and other hydrological features, including variability and changes in TWS. In addition, other human activities related to water resources management and practices such as dam release procedures and abstraction may also contribute to unique changes in local TWS (e.g., Ndehedehe et al., 2017b).

Nevertheless, our hypothesis in this study is that generally all the five global climate indices are linked to sub-seasonal and inter-annual patterns and anomalies of rainfall over Africa (cf. Figure 1). Hence, the same indices, at times individually or in combinations, could most likely have a significant influence on the variability of TWS at seasonal to inter-annual time scales over the continent. Therefore, one can consider the temporal patterns of the climate indices as known, and try to find similar patterns in TWS time series. This has been done here by computing linear correlations that are described in the next section along with a brief description of the different datasets used in this study.

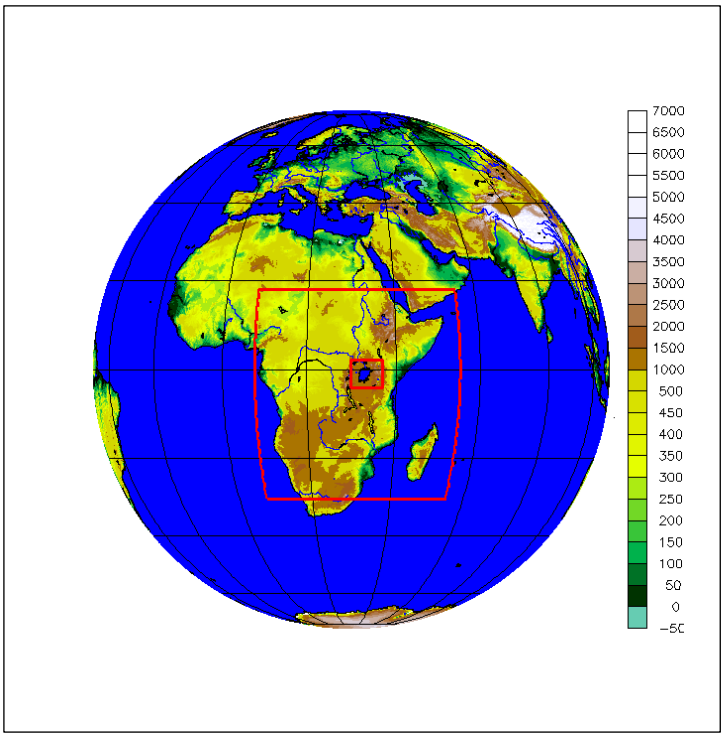

Figure 1 Study domain. Interior boxes feature sub-Saharan Africa (SSA) and Lake Victoria Basin (Largest Freshwater surface in Africa). The colors show elevation in meters.

3.0 Data and Methods

The data used include; monthly time series of GRACE-TWS, NOAA's Multivariate ENSO Indices (MEI), IOD data from Japanese Agency for Marine Earth-Science Research and Technology (JAMSTEC), QBO and NAO indices (from NOAA archive). Detailed descriptions of these data sets are presented in what follows.

3.1 Gravity Recovery And Climate Experiment (GRACE)

The GRACE mission, launched in 2002, is a joint US National Aeronautics and Space Administration (NASA) and the German Aerospace Centre (DLR) gravimetric mission aimed at providing spatio-temporal variations of the Earth's gravity field. On time scales ranging from months to decades, temporal variations of gravity are mainly due to redistribution of water mass in the surface fluid envelopes of the Earth. Over land, GRACE provides measurements of vertically integrated terrestrial water storage (TWS) changes, which include surface water, soil moisture, groundwater, snow over large river basins, and biomass (see, e.g., Tapley et al., 2004). Monthly GRACE-TWS data used in this study were obtained from the German Research Centre for Geosciences Potsdam (GFZ). Version (RL05a) of GRACE level-2 data (1^0x 1^0 spatial resolution) from GFZ that are derived in terms of fully normalized spherical harmonic (SH) coefficients of the geopotential fields up to degree and order 90 were downloaded from the Information System and Data Centre (ISDC) (http://isdc.gfz-potsdam.de/index.php) and used to compute monthly TWS fields. First, GRACE Level-2 solutions were augmented by the degree-1 (https://grace.jpl.nasa.gov/data/get-data/geocenter/) in order to include the variation of the Earth's center of mass with respect to a crust-fixed reference system. This replacement is undertaken due

to its impact on the amplitude of the annual and semi-annual water storage changes. Degree 2 and order 0 (C20) coefficients from GRACE (Cheng et al., 2014; Khaki et al., 2017a; Khaki et al., 2017b) are not well determined and were replaced using JPL products (http://grace.jpl.nasa.gov/data/get-data/oblateness/).

GRACE level-2 spherical harmonics at higher degrees are affected by correlated noise (e.g., Khaki et al., 2018) and are therefore filtered using the DDK3 de-correlation filter (similar to that of Kusche et al., 2009). Selecting DDK3 for filtering GRACE products makes a good sense since GFZ RL05a data represents considerably lower noise than the previous release of the GRACE level-2data. Monthly DDK3 filtered solutions were then used to generate TWS grids over Africa following the approach of Wahr et al., (1998). Since the signals over land areas are of interest to this study, the ocean areas were masked using a sea-land mask similar to the mask that is used to generate GRACE-AOD1B de-aliasing products (http://www.gfz-potsdam.de/AOD1B).

3.2 Global Climate Indices

3.2.1 Multivariate ENSO Index (MEI)

MEI (http://www.esrl.noaa.gov/psd/enso/mei/) is the first principal component of the combined, normalized fields of sea level pressure, zonal and meridional components of wind, surface air pressure, and total cloudiness fraction. The units of MEI are standardized and hence a score of 1 represents a full standard deviation departure of the principal component for the respective season involved (Wolter and Timlin, 2011). A comparison of MEI and Nino3.4 indices in this study found the negligible difference between the correlation values computed (as will be demonstrated in the results discussed later in this contribution). NOAA's monthly MEI (2003 to 2014) is utilized in this study, where they are correlated with TWS time series over the same time period.

3.2.2 Indian Ocean Dipole (IOD) Index

Indian Ocean Dipole (IOD) is an irregular oscillation of sea-surface temperatures, in which the western Indian Ocean becomes alternately warmer or colder than the eastern part of the ocean. It is represented by anomalous SST gradient between the western equatorial Indian Ocean and the southeastern equatorial Indian Ocean, where this gradient is often referred to as Dipole Mode Index (DMI). In this study, the instantaneous and lagged monthly correlations between DMI (http://www.jamstec.go.jp/frcgc/research/d1/iod/HTML/Dipole%20Mode%20Index.html) and TWS data over the period 2003-2014 are analyzed.

3.2.3 Quasi-Biennial Oscillation (QBO) Index

QBO (http://www.esrl.noaa.gov/psd/data/correlation/qbo.data) involves the fluctuation between equatorial westerly and easterly wind regimes in the lower stratosphere with a period of about 26-29 months. This oscillation is discerned through an index that is based on a calculation of zonal wind anomaly at 30hPa averaged along the equator (u-30 QBO) or at 50hPa (u-50 QBO). Lau and Shoo (1988) suggested the link between the easterly phase of QBO and ENSO. In the

present study, QBO zonal index computed from NCEP/NCAR Reanalysis data at 30hPa level (i.e. u-30 QBO) covering the period 2003-2014 is utilized.

3.2.4 Madden-Julian Oscillation (MJO) index

The Madden-Julian Oscillation (MJO; Madden and Julian 1971, 1972) is a tropical atmospheric phenomenon first recognized in the early 1970s and is also commonly known as the 40-day wave. This wave often develops over the Indian Ocean and then travels east across the tropics at 5-10 m/s. The MJO has been suggested as a key factor in connecting or bridging weather and climate, and thus at times very important in influencing rainfall over eastern Africa, including the Lake Victoria Basin (see, e.g., Omeny et al., 2008). The MJO data used in this study was obtained from Climate Prediction Center (CPC) archive for the period 2003-2014 (http://www.cpc.noaa.gov/products/precip/CWlink/daily_mjo_index/mjo_index.html).

3.2.5 North Atlantic Oscillation (NAO) Index

The NAO (http://www.cpc.ncep.noaa.gov/products/precip/CWlink/pna/nao.shtml) consists of a north-south dipole of anomalies, with one center located over Greenland and the other center of opposite sign spanning the central latitudes of the North Atlantic between 35^{o}N and 40^{o}N. Both negative and positive phases of the NAO are associated with basin-wide changes in the intensity and location of the North Atlantic jet stream and storm track and in large-scale modulations of the normal patterns of zonal and meridional heat and moisture transport, which in turn results in changes in global temperature and precipitation patterns. NAO data for the period 2003-2014 was employed in this study.

4.0 Results and Analysis

The key findings of the present study are presented as follows: The Pearson correlations between the five global climate indices (time series) and GRACE-TWS are presented in sections 4.1 and 4.2, in which instantaneous and lagged linear relations are discussed. In section 4.3, the lagged relationships are explored further after removing the seasonal (annual and semi-annual cycles) from both indices and GRACE TWS products in order to ensure that any seasonal dependence of this variability that might also be linked to the dominant seasonal rainfall patterns over Africa has been accounted for. In section 4.4, a reduction of the redundant information between climate indices is discussed based on the statistical technique of Independent Component Analysis (ICA, see e.g., Forootan and Kusche, 2012 and 2013). In light of this analysis, a correlation analysis is performed in section 4.5 between the dominant independent patterns of climate indices and GRACE-TWS changes. In order to provide a measure of an average influence of each climate index on TWS changes over the period of our study, the normalized time series of each index along with a linear trend and annual/semi-annual cycles are fitted to the time series of TWS changes in each grid as:

$$x(i,j,t) = a + bt + c\sin(2\pi t) + d\cos(2\pi t) + e\sin(4\pi t) + f\sin(4\pi t) + gI + hH(I(t)) + \varepsilon(t) \quad \text{Eq (1)},$$

where i and j represent the location of the grid, t is time in years, $H(I(t))$ represents a Hibert transformation of the normalized climate index, which is the same as I but after shifting by $\pi/2$ in the spectral domain, and $\varepsilon(t)$ represents the temporal residuals. Coefficients a to h are

computed using the least squares approach. The influence of the five global climate indices on TWS variability is then examined to identify possible "hot-spots", where changes in TWS are significantly influenced by a specific or a combination of the indices (i.e., ENSO, IOD, QBO, MJO, and NAO), and whether there exists phase-locked or lagged relationships. In the following sections the influence of g that also indicates the possible contributions of each index (or their combinations) in TWS changes are presented.

4.1 Instantaneous Pearson Correlation and Amplitude Analysis.

Instantaneous correlations (lag-0) between the five climate indices and TWS during the period 2003-2014 are presented in Figure 2. Note that the amplitudes of the r-values indicate whether the effect of a particular climate index represents positive or negative change in monthly TWS (e.g., Figure 2 A2-E2). The amplitude of each index (g in Eq. (1)) is shown in millimeters (mm) i.e., the middle panels of Figure 2 (A2-E2). The statistical significance of their-values at 95% confidence level are presented on the right panel (A3-E3), where zero (0) indicates non-significant correlations and 1 is significant. The correlation analysis is undertaken considering different levels of noise in TWS data. Values between 0 and 1 in the right panel indicate regions where the estimated correlations are accepted when the noise level is less than 1 cm, and they are rejected when the noise levels are considerably higher.

GRACE- TWS and ENSO are highly correlated (positive) primarily along the western coast of the Indian Ocean/East Africa coast (Figure 2: A-1). Also, positive correlations between ENSO and TWS occur along the West African coast, especially coast of Guinea, in the Mediterranean, as well as over central parts of the Sahel. These findings support the work of Ndehedehe et al., (2017), which found strong presence of ENSO-induced TWS derived from MERRA reanalysis data in the coastal West African countries and most of the regions below latitude 10° N. However, TWS and ENSO are mostly negatively correlated over central Africa (especially over the Congo Basin/Forest) and parts of South Africa, western Ethiopia and most parts of Sudan. The correlations are significant over the coastal regions of the Horn of Africa although the amplitudes (mm) are fairly low (Figure 2: A-1 - A-3). Over the equatorial central/eastern Africa and the coast of Guinea, however, the amplitudes are greater than 10 mm/month implying that ENSO-related precipitation induces an increase of about 10 mm/month or more in TWS (Figure 2: A-2).

Pearson correlations between IOD and TWS reveal a unique dipole correlation pattern with strong positive correlations with amplitudes exceeding 10 mm/month over the southern margins of the Sahel, but large negative correlations (with amplitude less than -10mm/month) are dominant over central and eastern Africa, and particularly over the Congo Basin (Figure 2:B-1 and B-2). It is notable that over equatorial eastern Africa, these correlations are somehow opposite to the expected wet/dry anomalies associated with positive/negative IOD phases (e.g., Saji et al., 1999), which might be due to the short period of the dataset used in the present study. However, several other factors including the complex terrain over East Africa can influence the spatial organization of surface and sub-surface water patterns in return leading to TWS patterns that may be inconsistent with known IOD-rainfall relationships.

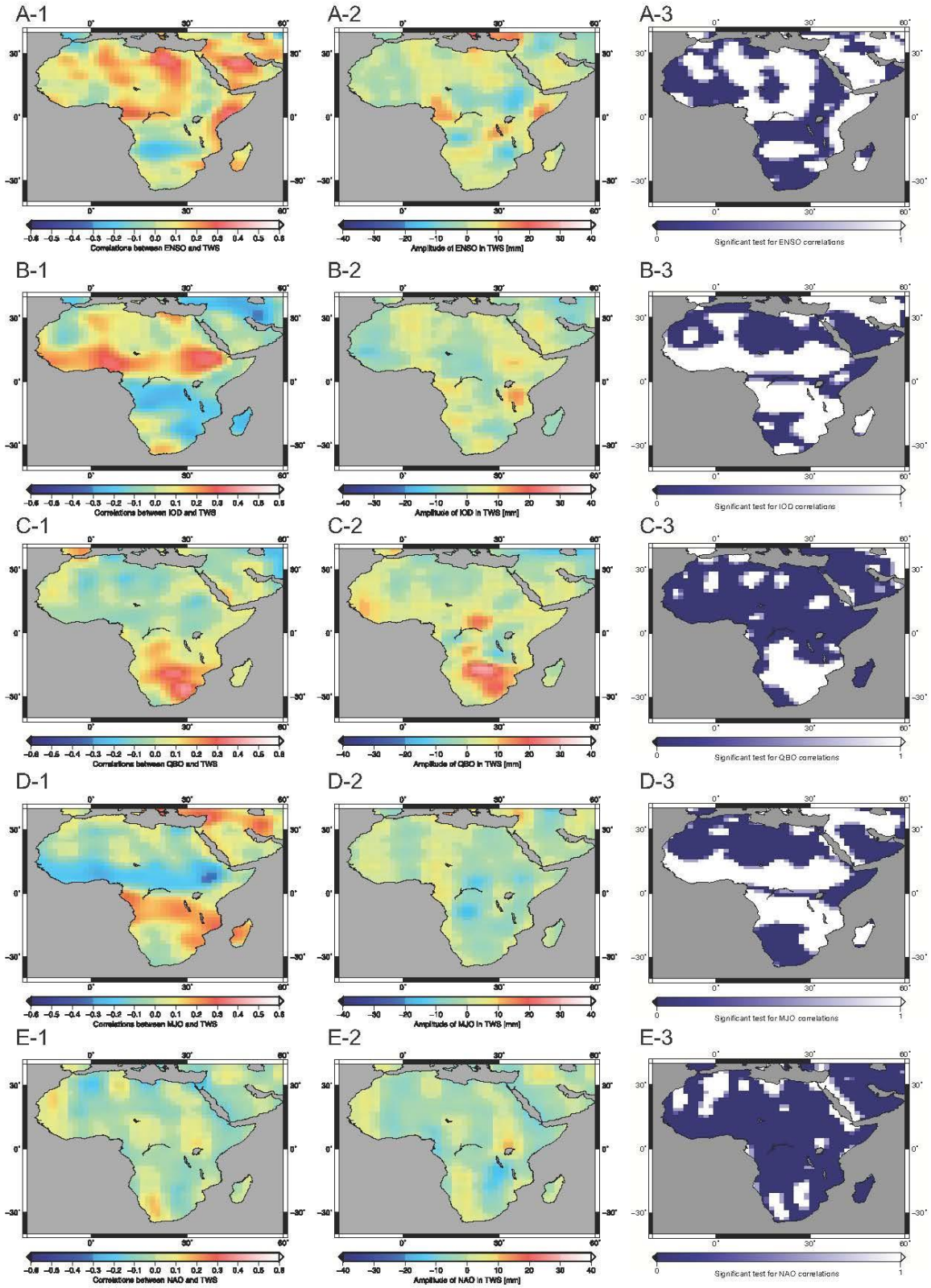

Figure 2 correlations between the five climate indices and TWS during the period 2003-2014 (A-1-E-1), the amplitude of each index (A-2-E-2), and the statistical significance of the r-values at 95% confidence level (A-3-E-3).

Statistically significant, positive, correlations between QBO and TWS are also found over southern Africa (Figure 2: C-1, C-2, and C-3). However, the impact of MJO on monthly TWS changes over Africa is dominated by a dipole pattern, characterized by large negative r-values over southern margins of the Sahel (Figure 2: D-1 to D-3), extending into western Ethiopia and over the coast of West Africa, and large positive r-values over equatorial central Africa/Congo Basin and southwestern coast of Indian Ocean (i.e., southern parts of East Africa extending into Tanzania and Mozambique). In contrast, the NAO index apparently displays no strong influence on TWS changes over Africa (Figure 2:E-1 to E-3) based on instantaneous correlations with monthly data.

4.2 Lagged Pearson Correlations and Amplitude Analysis

To examine if there existed any lagged relationships between TWS changes and the five global climate indices given the fact that for hydrological processes, a temporal lag usually exists between changes in fluxes (precipitation, evapotranspiration, and runoff) and the peak of water storage (see e.g., Awange et al., 2013), lagged Pearson correlation analysis is done (e.g., Figure 3). Furthermore, global climate teleconnections such as ENSO often lead to shifts in global climatic patterns such as east-west displacement of the Walker circulation over equatorial eastern and central Africa that might impose lead/lag time of up to 6 months (e.g., Indeje et al., 2000). Hence, ENSO could as well affect the seasonal and inter-annual variability of TWS. In Figure 3:A-1, our results show that most regions (north of15^{o}S) apparently display very strong lagged relationships/correlations between ENSO and TWS that include an 8-12 and 4-8 month lagged relationships over the Sahel and equatorial eastern Africa, respectively (Figure 3:A-3). However, significant negative correlations between ENSO and TWS over southern Africa appear to be more phase-locked (lag=0). But, unique lagged relationships between TWS and IOD are found particularly over equatorial eastern (around Lake Victoria Basin) and central Africa, where the amplitudes of the influence are found to be greater than 20 mm/month especially within 2-6 month lags (Figure 3: B-2, B-3, B-4).

The lagged correlations computed between QBO index and TWS display fairly strong positive relationship over southern Africa (Figure 3: C-1) especially with 2-month lag (Figure 3: C-3). However, very low (insignificant) QBO-TWS correlations exist over the rest of sub-Saharan Africa as shown in Figure 3: C-4. One of the possible reasons is that QBO time scale is in the intervening period between that of ENSO (3-5 yrs) and IOD (2-5 yrs) and hence the QBO is highly likely masked by the stronger ENSO and IOD signal given also that our study period covered only 10 years.

In Figure 3: D, the relationships between MJO and TWS are explored. It should be noted that even though the periodicity of MJO is approximately 30-90 days, we believe that the monthly time series of TWS and MJO index covering the 13-year period of our study is long enough to capture the right phases of MJO and possible relationships with TWS changes. As a whole, the MJO index is found to be positively/negatively correlated with TWS over northern sub-Saharan Africa/southern Africa (Figure 3: D-1), with MJO-TWS relationship over southern Africa appearing to be strong within 6-8 months lag (Figure 3: D-1, D-3). The amplitudes of the influence are however considerably smaller than other induces (compare Figure 3: D2 with other plots on the same column).

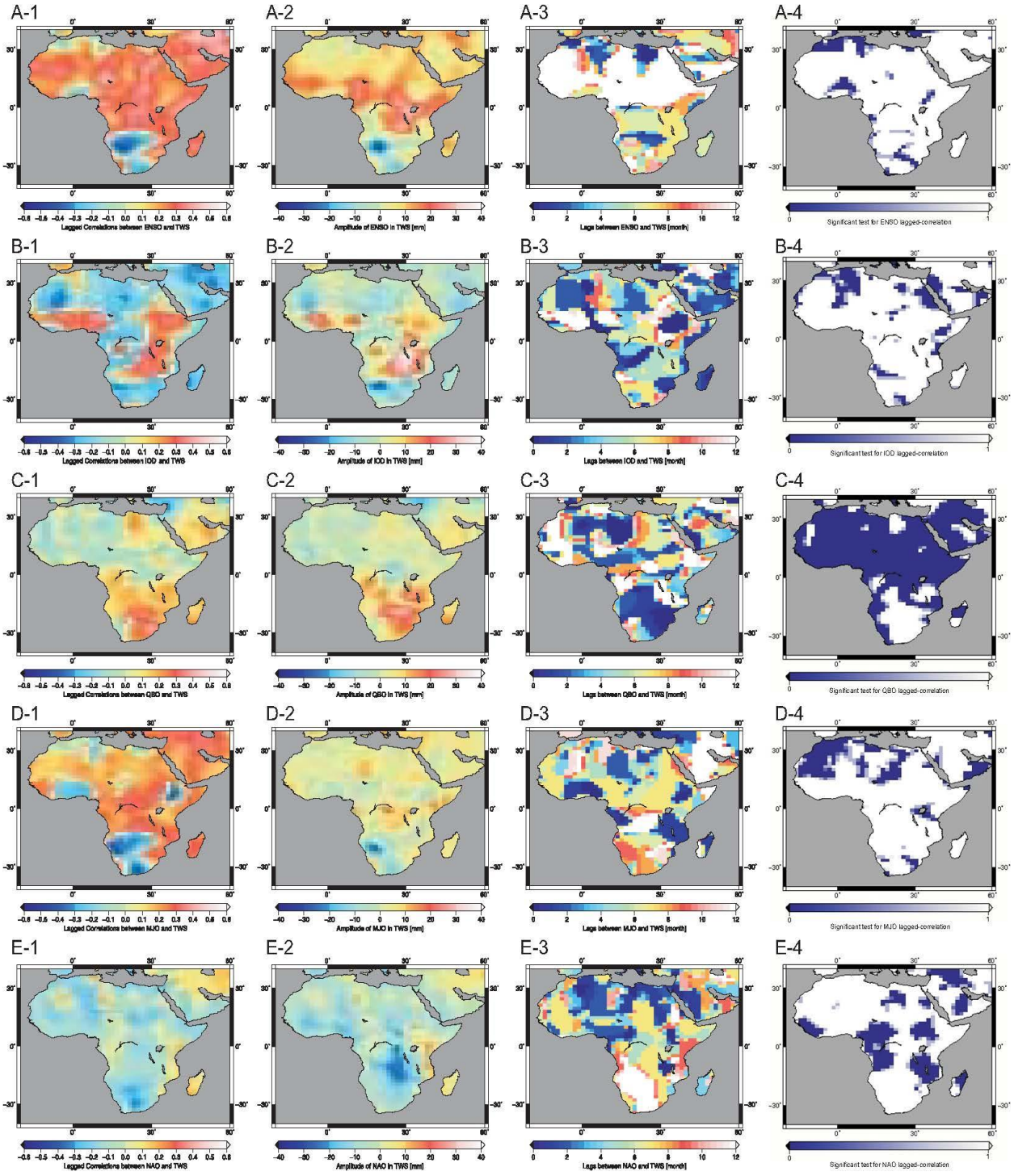

Figure 3 lagged correlations between the five climate indices and TWS (A-1-E-1), the amplitude of each index (A-2-E-2), 2-month time lag between the indices and TWS (A-3-E-3), and the statistical significance test for lagged-correlation (A-4-E-4).

With regard to the potential relationships between NAO and TWS variability over sub-Saharan Africa, our analysis reveals that the only regions where significant lagged correlations exist are

over the western part of southern Africa. The r-values over these regions are also significant at 95% confidence level, especially at 8-12 month lag (Figure 3: E-3 and E-4).

To ensure that the results described above are robust enough, we perform further analysis of the correlations between TWS and climate indices after filtering out seasonal cycle (semi-annual and annual cycles) from the monthly time series of the five indices. Part of the reason for doing this is due to the dominant role of ITCZ that drives the seasonality of climate, especially rainfall over Africa. The results are discussed in detail in the next section.

4.3 Lagged Correlation and Amplitudes after Filtering Annual and Semi-annual Cycles

The north-south migration of ITCZ and external forcing associated with global atmospheric circulation and sea surface temperature (SST) perturbations (e.g. Giannini et al., 2003) has been shown to be partly responsible for the strong seasonal variability of precipitation over Africa. We investigate if the variability of TWS is also in synch with the seasonal and inter-annual variability of precipitation, in response to five global teleconnection indices. Generally, the correlations between the five indices (ENSO, IOD, NAO, MJO, QBO) and TWS are relatively stronger, with annual/semi-annual cycles filtered from the time series, suggesting apparent climate-TWS association at inter-annual scale (see Figure 4). For instance, in Figure 4: A-1 to A-4, the correlation between ENSO and TWS is found to be more significant over many parts of Africa when the seasonal cycle is filtered from the ENSO index, compared to cases where seasonal cycle is unfiltered(cf. Figure 3: A-1) although the spatial patterns remains the same. This implies that strong ENSO-TWS relationship is more pronounced when semi-annual and annual cycles are filtered. However, statistically significant ENSO-TWS r-values greater than 0.4 (using 137-month time series: 2003-2013) tended to occur with 6 to 12 months lags, especially over the Sahel and the Horn of Africa (Figure 4: A-3 and A-4).

Similarly, the IOD-TWS relationships after annual/semi-annual cycles are filtered also depict very strong lagged correlation (more than 0.4 with lags of 2 to 6 months), particularly over equatorial central Africa and Lake Victoria Basin in eastern Africa (Figure 4: B-1 to B-4). However, areas depicting strong QBO influence on TWS at inter-annual and longer time scales tend to be confined mostly over southern Africa (Figure 4:C-1 to C-4). MJO-TWS relationship is presented in Figure 4: D-1 to D-4, which shows strong relationship over southern Africa within 6-8 months lags (see also Figure 2: D). Finally, the potential NAO-TWS relationships through lagged correlation after filtering the seasonal cycle from the time series tend to be dominated by very large negative correlations over southern Africa (Figure 4: E-4), but virtually uncorrelated over the rest of the continent.

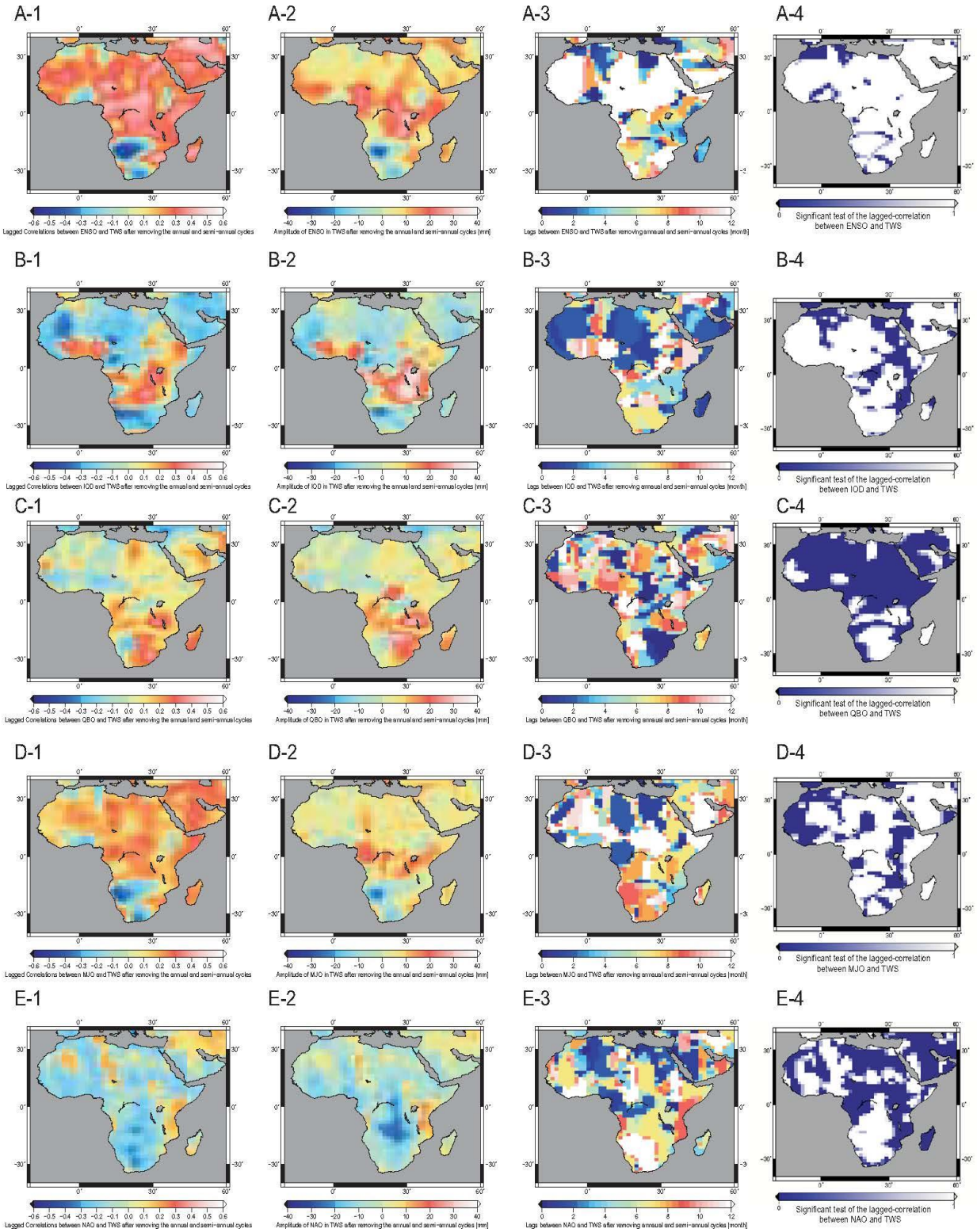

Figure 4 Lagged Correlations between the five indices and TWS (A-1-E-1), the amplitude of each index A-2-E-2), lags between the indices and TWS A-3-E-3), and the statistical significance test for lagged-correlation (A-4-E-4). Note that annual and semi−annual cycles are removed before these processes.

Overall, both lagged and instantaneous correlations between individual climate indices (CI) and TWS produce unique regions, where the CI-TWS connections/relationships are very strong (see Table 1 for a summary). This is the same for cases both with and without the semi-annual and annual cycles filtered from the time series of the climate indices during the 137-months' period, spanning 2003-2013. In addition, it is worth noting that for some indices (e.g., ENSO and IOD), the interpretation of possible physical processes/drivers linked to their TWS relationships must be done with caution. This is due to the fact that ENSO and IOD are sometimes highly interrelated, posing challenges in separating their unique and/or combined influences on regional or continental precipitation and TWS patterns. In other words, isolating their unique/combined contributions (correlation) to TWS variability at monthly, seasonal, inter-annual and longer time scales is challenging. Hence, in the next section, the statistical interdependence between/among climate indices are accounted for using Independent Component Analysis (ICA, Forootan and Kusche, 2012, 2013).

Table 1: Summary of the influence of global indices on TWS

Index/Mode	Impact on TWS	Regions with the strong CI-TWS relationship	Remark
ENSO	Negatively correlated Positively correlated	Southern Africa Eastern Africa Sahel	No lag No lag 6-12 month's lag
IOD	Positively correlated	Eastern Africa Central Africa (Congo Basin)	2-6 month's lag
QBO	Positively correlated	Southern Africa	2 month's lag
MJO	Positively correlated	Congo Basin Southern Africa	No lag 4-6 month's lag
NAO	Positively correlated	Southern Africa	6-8 month's lag

4.4 ICA-derived Isolation of Redundant Information Between Climate Indices

ICA is applied to the time series of climate indices in order to explore the existence of any significant modes of monthly and inter-annual variability of TWS over Africa that may be linked to specific or combined global climate indices (see Table 2). The time series of the three leading Independent Components (ICs) are retained and correlated with respective time series of the five climate indices. From a statistical point of view, ICA technique makes use of the higher order (higher than second order mutual statistical information) between climate indices to extract modes that are statistically mutually as independent as possible (see Forootan, 2014 for more details). Applying ICA is equivalent to defining a linear relationship (shown by a mixing matrix **A**) between observations (available CIs stored in matrix **X**) and temporally independent components ICs (stored in matrix **S**)

$$\boldsymbol{X} = \boldsymbol{AS}.$$

Here **A** is computed by making the fourth-order cumulant's tensor based on the time series of CIs as diagonal as possible as outlined in Forootan and Kusche (2012).

In Figure 5, the correlation matrix of the estimated Independent Components (ICs) from the climate indices (CIs) versus individual climate indices is presented, and generally, the ICA technique is able to isolate the redundant information between CIs well. The first ICA mode (IC1) is seen to be highly correlated with NAO (positive), while the second ICA mode (IC2) is highly correlated to ENSO (negative) and modestly correlated to MJO (negative). IC3 is highly correlated with QBO (negative). Therefore, no duplicated correlations are seen between ICs and the indices (i.e., no climate index is correlated with more than one IC, see Figure 5). This means that the leading modes of ICA have the potential to distinguish between the unique or combined contributions/relationships of the global climate indices and TWS changes. We also note that none of the ICs are correlated with IOD. Tables 3 show the actual correlation while Figure 5 provides a visual clarity.

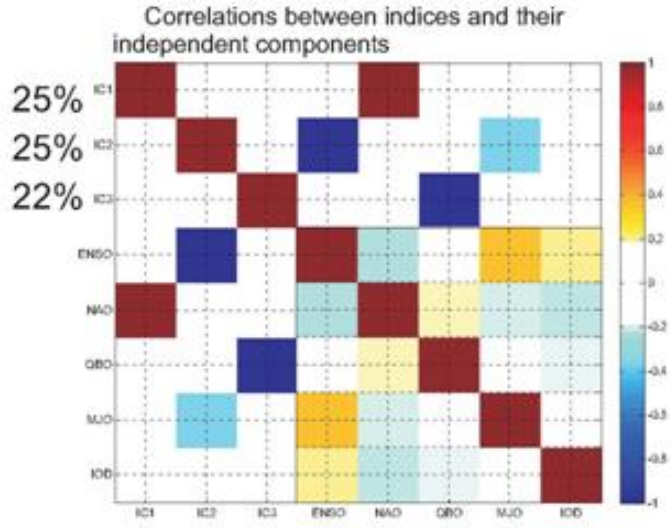

Figure 5 Correlation between the indices and their Independent Components

Table2: A summary of the influence of the leading Independent Components (ICs) on TWS

ICA Mode	Impact on TWS	Regions with strong IC-TWS relationship/correlation	Remark
IC1	Reduction in TWS	Eastern Africa Southern Africa	Greater than 10mm/month reduction Occurs 6-8 month's lag
IC2	Reduction in TWS	Sahel, Central Africa	-
IC3	Unclear influence	All sub-Saharan Africa	-

Table 3: Correlations (at 95% confidence level) between leading Independent Components and global climate indices

IC1	1							
IC2	0.01	1						
IC3	-0.1	0.0	1					
ENSO	0.01	-0.8	0.0	1				
NAO	0.9	0.0	0.0	-0.3	1			
QBO	0.1	0.0	-0.8	0.0	0.2	1		
MJO	0.1	-0.3	-0.1	0.4	-0.2	0.0	1	
IOD	0.01	0.01	0.0	0.2	-0.3	-0.2	0.0	1
	IC1	IC2	IC3	ENSO	NAO	QBO	MJO	IOD

4.5 Correlations between Leading ICA Modes of Climate Indices and GRACE-TWS

The lagged correlations between IC1 and TWS, after removing the seasonal cycles, are shown in Figure 6: A-1. The large negative r-values over southern and equatorial Africa (especially over the Congo Basin), also co-located with regions of reduced TWS of 10mm/month or less are very conspicuous. The r-values also tended to be larger (negative; <-0.4) and significant at 6-12 months lags. This likely implies that the influence of NAO on TWS (see, Figure 5-B) is very strong over parts of southern Africa and the Congo Basin (Figure 6: A-3 and A-4) several months after the peak NAO events. The lagged correlations between IC2 and TWS, after filtering semi-annual cycle from TWS time series (Figure 6: B-1) most likely represent a combined ENSO and MJO influence on TWS changes over parts of Africa.

Generally, large negative correlations are found over equatorial central Africa/Congo Basin and most parts of the Sahel. The higher (negative) IC amplitudes (mm) are also co-located with regions of higher r-values (Figure 6:B-2). The r-values are statistically significant over the Sahel, especially at 6-8 months lag. This apparently implies that ENSO-related hydroclimate anomalies tend to reduce TWS over these areas (especially over the Sahel) long after the peak of the ENSO episodes (Figure 6: B-3 and B-4). This ENSO-TWS relationship does not seem to mimic the often-witnessed ENSO-rainfall wet/dry dipole pattern over eastern/southern Africa (e.g., Indeje et al., 2000). This probably implies two points: first there are completely unique regions with very strong ENSO-TWS relationships, and secondly the time lags for ENSO influence on TWS are completely different from those of ENSO-rainfall relationship. Finally, in Figure 6: C-1, the lagged correlations between IC3 and TWS are shown. It should be noted that as shown earlier (Figure 5) IC3-TWS correlations represents an apparent influence of IOD on TWS. However, comparing r-values and the amplitudes of IC3 (Figure 6: C-2) and the t-statistics map (Figure 6:C-4),the potential influence of IOD on TWS variability clearly emerges only over southern

Africa. A summary of the correlation results between climate indices/their independent components and TWS changes of Africa over 2003-2014 are summarized in Table 1.

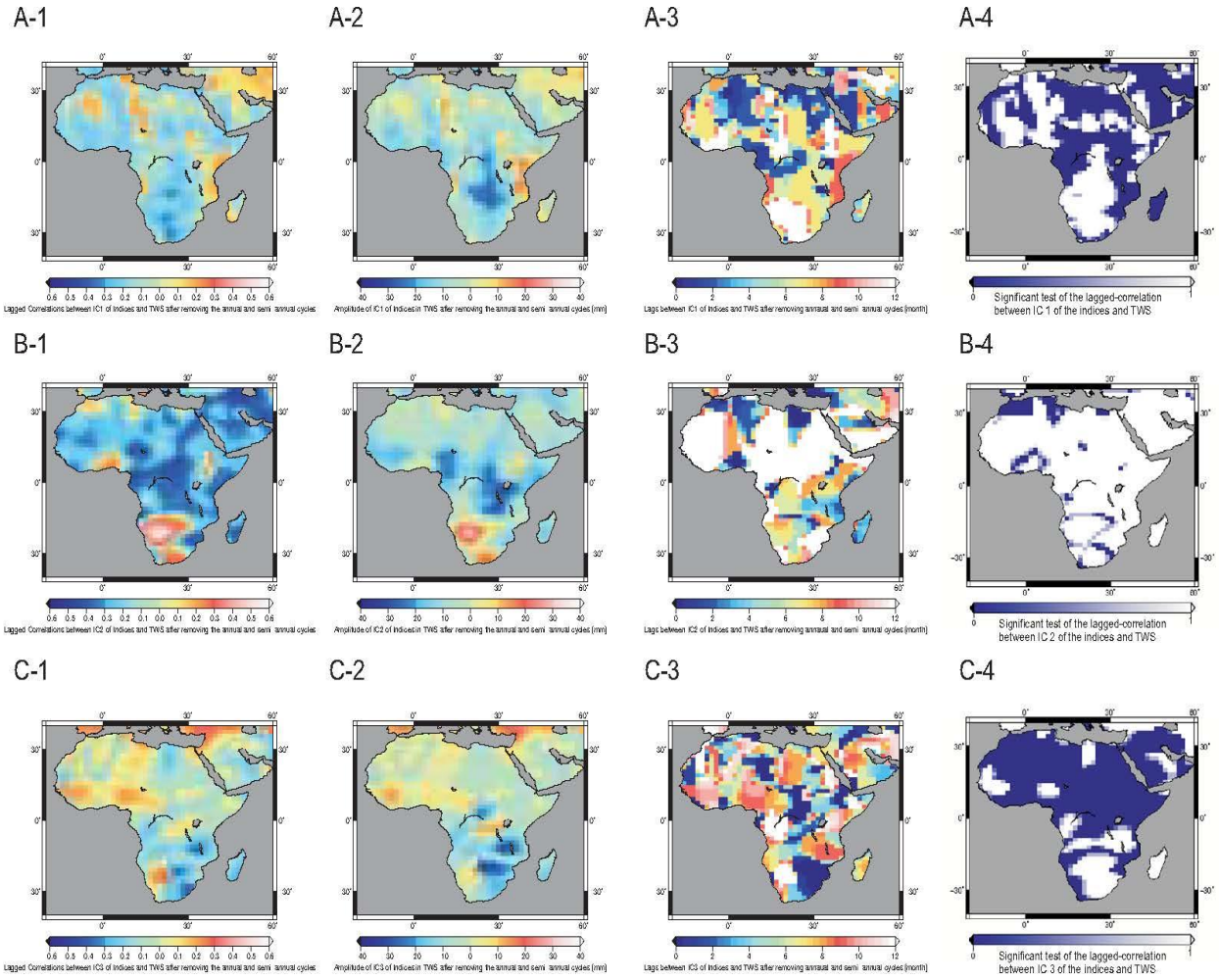

Figure 6 Lagged Correlations between the five indices Independent Components (ICs) and TWS (A-1-E-1), the amplitude of each index's IC (A-2-E-2), lags between the ICs of indices and TWS (A-3-E-3), and the statistical significance test for lagged-correlation (A-4-E-4). Note that annual and semi–annual cycles are removed before these processes.

5.0 Conclusions

The potential influence of five key global climate teleconnection indices or indicators on total water storage (TWS) over Africa was investigated through Pearson correlation analysis. Independent Component Analysis (ICA) technique is employed to isolate potential contributions/relationships between individual or combined global climate indices on GRACE-derived TWS changes. Our analysis is mostly focused on the period, 2003-2014, during which more than 10-years of GRACE-derived TWS data with a moderate level of noise is available.

First, temporal Pearson correlations between individual climate indices and TWS data were computed to provide a first-order assessment and identify unique regions where the climate

indices might significantly impact TWS changes at monthly (sub-seasonal) or longer (inter-annual) time scales. Second, in order to account for the effect of the seasonality of the global indices and potential links to TWS variability, lagged correlations between ICs and TWS after filtering the annual and semi-annual cycles from the time series of climate indices were performed.

Whereas it is obvious that a complex mix of processes may dictate the associations between the global climate teleconnections and continental terrestrial water storage changes, the present study focused mainly on the potential relationships and influence of specific/combined climate indices on TWS changes. As such, it should be noted that some of the confounding factors, not fully considered in our analyses, including e.g., the role of complex terrain especially over the equatorial and the Horn of Africa that potentially can influence surface and sub-surface hydrological processes including changes in the groundwater storage, which in return influences the space-time variability of TWS. Other human-induced activities such as land use patterns and surface/groundwater usage/abstraction might also influence TWS changes but are not necessarily related to possible influences of global climate indices or teleconnections. Finally, it should also be noted that isolating the physical mechanisms through which specific/combined global climate indices might influence TWS changes was beyond the scope of the present study. Instead, the study focused on isolating the possible influence of global climate indices and/or teleconnections on TWS over Africa based primarily on first order statistical correlations and ICA decompositions.

Based on Pearson correlation and ICA analyses, the study:

1. Revealed *unique relationships* between TWS and specific global climate indices. In certain cases the regions with the strong CI-TWS connection, e.g. where the indices had significant influences on TWS changes corresponded to areas where previous studies have demonstrated the strong influence of the indices on rainfall anomalies. For, instance, ENSO tended to have a phase-locked positive relationship with TWS over equatorial eastern Africa, consistent with the ENSO-rainfall relationship over the region.
2. Revealed *unique regions* where CI-TWS relationships were very strong and thus where specific/combination of climate index/indices tended to have a very significant influence on the spatio-temporal variability and changes of TWS. For, example, the apparent ENSO-related influence tended to reduce TWS over certain areas especially over the Sahel with nearly a 6-8 months' time lag. Also, an apparent combined ENSO/MJO negative impact on TWS over equatorial central Africa/Congo Basin and most parts of the Sahel was consistently identified. In addition, NAO seemed to have a significant 6-10 months lagged impact (increase) on TWS over parts of southern Africa and the Congo Basin.
3. The Pearson correlations and the independent components of climate indices are found to be able to somehow isolate possible contributions (correlations) of single or combined climate indices to TWS changes.
4. NAO was highly correlated with the leading ICA mode (IC1) over parts of southern Africa and southern Congo Basin. On the one hand, this implied that NAO tended to influence TWS variability over these regions, especially with a time lag of 6-8 months. On the other hand, the lagged correlations patterns between the second ICA mode (IC2) and TWS apparently indicated strong relationships between combined ENSO/MJO

indices and TWS changes, with large negative correlations located over equatorial central Africa/Congo Basin and most parts of the Sahel, mostly at 8-12 months' time lag.

5. Finally, strong lagged correlations between the third ICA mode (IC3) and TWS were stronger over southern Africa and apparently linked to influence of QBO on TWS over the region.

Acknowledgments

R. Anyah was supported by US National Science Foundation through Grant #: AGS-1305043. J. Awange appreciates the financial support of Alexander Von Humboldt foundation that supported his stay at Karlsruhe Institute of Technology (KIT), Karlsruhe, Germany. E. Forootan is grateful for the financial supports by the German Aerospace Center (DLR) under the project (D-SAT project - Fkz.: 50 LZ 1402), and the WASM/TIGeR research fellowship from Curtin University. M. Khaki is grateful for the research grant of Curtin International Postgraduate Research Scholarships (CIPRS)/ORD Scholarship provided by Curtin University. The authors are grateful to the GFZ and NASA, and NOAA for providing the GRACE satellite and Global Climate Indices data for this study.

6.0 References

AghaKouchak, A. (2015), A multivariate approach for persistence-based drought prediction: Application to the 2010-2011 East African Drought, Journal of Hydrology, 526, 127-135.

Agola N. O and Awange J. L. (2014) Globalized Poverty and Environment 21st Centur challenges and Innovative Solutions. Springer, Berlin, New York.

Agutu, N.O., J.L. Awange, A. Zerihun, C.E. Ndehedehe, M. Kuhn, Y. Fukuda, (2017), Assessing multi-satellite remote sensing, reanalysis, and land surface models' products in characterizing agricultural drought in East Africa, Remote Sensing of Environment, Volume 194, Pages 287-302, ISSN 0034-4257, https://doi.org/10.1016/j.rse.2017.03.041.

Anderson, W. B., B. F. Zaitchik, C. R. hain, M. C. Anderson, M. T. Yilmaz, J. Mecikalski, Schultz, L. (2012), Towards an integrated soil moisture drought monitor for East Africa, Hydrology and Earth System Sciences, 16, 2893-2913.

Anyah, R. O. and Semazzi F. H. M. (2004), Simulation of the sensitivity of Lake Victoria basin climate to lake surface temperatures. Theoretical and Applied Climatology, 79, 55-69.

Anyah, R.O., Semazzi F. H. M., L. Xie (2006), Simulated physical mechanisms associated with climate variability over Lake Victoria Basin in East Africa. Mon. Wea. Rev., 134, 3588–3609

Anyah R.O., and Semazzi F.H.M (2007), Variability of East African rainfall based on multi-year RegCM3 model simulations. Int. J. Climatol.: 27, 357-371

Anyah, R.O., F.H.M. Semazzi, 2009: Idealized simulation of hydrodynamic characteristics of Lake Victoria that potentially modulate regional climate. International Journal of Climatology 29:7, 971-981

Awange J.L. and Ong'ang'a, O. (2006), Lake Victoria: Ecology Resource and Environment. Springer-Verlag, Berlin, Heidelberg, New York, 354p.

Awange J. L., Aluoch J., Ogallo L., Omulo M., and Omondi P. (2007), An assessment of frequency and severity of drought in the Lake Victoria region (Kenya) and its impact on food security. Climate Research 33 135-142.

Awange J L, Sharifi M A, Ogonda G, Wickert J, Grafarend E W and Omulo M A (2008), The falling Lake Victoria water level: GRACE TRIMM and CHAMP satellite analysis of the lake basin Water Resour. Manage. 22 775–96

Awange J.L, Anyah, R.O., Agola, N.O, Forootan, E., and Omondi, P.O. (2013), Potential impacts of climate and environmental change on the stored water of Lake Victoria Basin and economic implications. Water Resources Research: 49, 8160–8173, doi:10.1002/2013WR014350.

Awange J.L, Forootan, E., Kuhn M., Kusche J., Heck B (2014) Water storage changes and climate variability within the Nile Basin between 2002 and 2011. Advances in Water Resources 73 (2014) 1–15. http://dx.doi.org/10.1016/j.advwatres.2014.06.010.

Awange, J.L., Khandu, M. Schumacher, E. Forootan, B. Heck, (2016a), Exploring hydro-meteorological drought patterns over the Greater Horn of Africa (1979–2014) using remote sensing and reanalysis products, Advances in Water Resources, Volume 94, 2016, Pages 45-59, ISSN 0309-1708, https://doi.org/10.1016/j.advwatres.2016.04.005.

Awange, J. L., F.Mpelasoka, R. M. Goncalves, (2016b), When every drop counts: Analysis of Droughts in Brazil for the 1901-2013 period, Science of The Total Environment, Volumes 566–567, 2016, Pages 1472-1488, ISSN 0048-9697, https://doi.org/10.1016/j.scitotenv.2016.06.031.

Becker M, LLovel W, Cazenave A, Guntner A, Cretaux JF, (2010), Recent hydrological behavior of the East African great lakes region inferred from GRACE, satellite altimetry and rainfall observations, Compt. Rend. Geosci.,342(3), 223-233

Black E., J. Slingo, and Sperber K.R., (2003), An observational study of the relationship between excessively strong short rains in coastal East Africa and Indian Ocean SST. Mon. Wea. Rev., 31, 74-94.

Cao, Y.; Nan, Z.; Cheng, G. (2015), GRACE gravity satellite observations of terrestrial water storage changes for drought characterization in the arid land of Northwestern China. Remote Sens., 7, 1021–1047.

Clark, C. O., P. J. Webster, and J. E. Cole (2003), Interdecadal variability of the relationship between the Indian Ocean Zonal Mode and East African Coastal Rainfall Anomalies, Journal of Climate, 16, 548-554.

Creutzfeldt B., Guntner A., Vorogushyn S., Merz B. (2010), The benefits of gravimeter observations for modelling water storage changes at the field scale.Hydrol. Earth Sys. Sci. 14(9):1715-1730

Eicker, A., Forootan, E., Springer, A., Longuevergne, L., Kusche, J. (2016). Does GRACE see the terrestrial water cycle `intensifying'? Journal of Geophysical Research-Atmosphere, 121, 733-745, doi:10.1002/2015JD023808

Forootan, E., Kusche, J., Talpe, M.J., Shum, C.K., Schmidt, M. (2018). Developing a complex independent component analysis (CICA) technique to extract non-stationary patterns from geophysical time series. Surveys in Geophysics, doi:10.1007/s10712-017-9451-1

Forootan, E. (2014), Statistical Signal Decomposition Techniques for analyzing time-variable satellite gravimetry data, Ph.D. thesis, University of Bonn, Bonn, Germany.

Forootan E., Kusche J., Loth I., Schuh W-D., Eicker A., Awange J., Longuevergne L., Diekkrueger B., Schmidt M., Shum C.K., (2014a). Multivariate prediction of total water storage anomalies over West Africa from multi-satellite data. Surveys in Geophysics, 35, Pages 913-940, doi:10.1007/s10712-014-9292-0.

661 Forootan, E., and Kusche, J. (2013), Separation of deterministic signals, using independent
662 component analysis (ICA). Stud. Geophys. Geod. 57, 17-26, doi:10.1007/s11200-012-
663 0718-1.
664 Forootan, E., and Kusche, J. (2012). Separation of global time-variable gravity signals into
665 maximally independent components. Journal of Geodesy, 86 (7), 477-497,
666 doi:10.1007/s00190-011-0532-5.
667 Goddard, L., and N.E. Graham, (1999), Importance of the Indian Ocean for simulating rainfall
668 anomalies over eastern and southern Africa. J. Geophys. Res., 104, 19,099-19,116.
669 Indeje M, F.H.M. Semazzi, L.J., Ogallo, 2000: ENSO signals in East African rainfall seasons.
670 Int. J. Climatol 20: 19–46
671 Indeje, M., and Semazz, F.H.M., (2000), Relationships between QBO in the lower equatorial
672 stratospheric zonal winds and east African seasonal rainfall. Meteor. Atm. 73(3-4), 227-
673 244.
674 Khaki, M., Schumacher, M., J., Forootan, Kuhn, M., Awange, E., van Dijk, A.I.J.M., (2017a)
675 Accounting for Spatial Correlation Errors in the Assimilation of GRACE into
676 Hydrological Models through localization. Advances in Water Resources, 108:99-112,
677 doi:10.1016/j.advwatres.2017.07.024.
678 Khaki, M., Hoteit, I., Kuhn, M., Awange, J., Forootan, E., van Dijk, A.I.J.M., Schumacher, M.,
679 Pattiaratchi, C., (2017b). Assessing sequential data assimilation techniques for integrating
680 GRACE data into a hydrological model. Advances in Water Resources, 107:301-316,
681 doi:10.1016/j.advwatres.2017.07.001.
682 Khaki, M., Forootan, E., Kuhn, M., Awange, J., Longuevergne, L., Wada, W., (2018), Efficient
683 Basin Scale Filtering of GRACE Satellite Products, In Remote Sensing of Environment,
684 Volume 204, 2018, Pages 76-93, ISSN 0034-4257,
685 https://doi.org/10.1016/j.rse.2017.10.040.
686 Kurnik, B., P. Barbosa, and J. Vogt (2011), Testing two different precipitation datasets to
687 compute the standerdised precipitation index over the Horn of Africa, International
688 Journal of remote Sensing, 32 (21), 5947-5964.
689 Kusche, J., Schmidt, R., Petrovic, S., Rietbroek, R. (2009), Decorrelated GRACEtime-variable
690 gravity solutions by GFZ, and their validation using a hydrological model.Journal of
691 Geodesy, 83, 903–913. http://dx.doi.org/10.1007/s00190-0090308-3.
692 Kusche, J., Eicker, A., Forootan, E., Springer, A., Longuevergne, L. (2016) Mapping
693 probabilities of extreme continental water storage changes from space gravimetry,
694 Geophys. Res. Lett., 43, 8026–8034, doi:10.1002/2016GL069538.
695 Lau, K. and Shoo, P.J. (1988), Annual cycle, Quasi-Biennial Oscillation and Southern
696 Oscillation in global precipitation.Journal of Geophysical Research, 93, 10975-10988.
697 Lyon, B. (2014), Seasonal Drought in the Greater Horn of Africa and Its Recent Increase during
698 the March-May Long Rains, Journal of Climate, 27, 7953-7975.
699 Mpelasoka, F, J. L. Awange, R.MikoszGoncalves, (2017), Accounting for dynamics of mean
700 precipitation in drought projections: A case study of Brazil for the 2050 and 2070
701 periods, Science of The Total Environment, ISSN 0048-9697,
702 https://doi.org/10.1016/j.scitotenv.2017.10.032.
703 Naumann, G., E. Dutra, F. Pappenberger, F. Wetterhall, and J. V. Vogt (2014), Comparison of
704 drought indicators derived from multiple data sets over Africa, Hydrology and
705 EarthSystem Sciences, 18, 1625-1640.

Ndehendehe C, Awange J, Agutu N, Kuhn M, Heck B (2016) Understanding changes in terrestrial water storage over West Africa between 2002 and 2014. Advances in Water Resources 88: 211-230, doi: 10.1016/j.advwatres.2015.12.009.

Ndehedehe CE, Awange JL, Kuhn M, Agutu NO, Fukuda Y. (2017a) Climate teleconnections influence on West Africa's terrestrial water storage. Hydrological Processes.31:3206–3224. https://doi.org/10.1002/hyp.11237

Ndehedehe CE, Awange JL, Kuhn M, Agutu NO, Fukuda Y (2017b) Analysis of hydrological variability over the Volta river basin using in-situ data and satellite observations. Journal of Hydrology: Regional Studies 12: 88-110, doi: 10.1016/j.ejrh.2017.04.005.

Ndehedehea CE, Awange JL, Agutu NO, Okwuash O (2018) Changes in hydro-meteorological conditions over tropical West Africa (1980‑2015) and links to global climate. Global Planetary Change, doi: 10.1016/j.gloplacha.2018.01.020.

Ni, S., Chen, J., Wilson, C.R. et al. (2018) Global Terrestrial Water Storage Changes and Connections to ENSO Events. Surv Geophys, 39: 1, doi:10.1007/s10712-017-9421-7

Nicholson S.E, Kim, J.,1997: Relationship of ENSO to African rainfall. Int. J. Climatol 17:117–135

Nicholson, S. E. and Kim, J. (1997), The relationship of the El Ni˜no Southern Oscillation to African rainfall, Int. J. Climatol., 17, 117–135.

Nicholson S.E., Yin X., and Ba M. B. (2000), On the feasibility of using a lake water balance model to infer rainfall: An example from Lake Victoria. J. Hydrological Sciences, 45, 75–96.

Nicholson S.E., (1996), A review of climate dynamics and climate variability in Eastern Africa. The limnology, climatology and paleoclimatology of the Eastern Africa Lakes. Gordon and Breach, New York, 57pp.

Ogallo, L.J. (1988), Relationships between seasonal rainfall in East Africa and the Southern Oscillation', Int. J. Climatol., 8, 31–43.

Omeny P.A., Ogallo, L.A., Okoola, R.A., Hendon, H., and Wheeler, M., (2008), East African rainfall variability associated with the Madden-Julian Oscillation. J. Kenya Meteorol. Soc., 2(2) 105–114.

Omondi P, OgalloAwange, J, Ininda J, Forootan E. The influence of lowfrequency sea surface temperature modes on delineated decadal rainfall zones in Eastern Africa region. Adv. Water Resour 2013. dx.doi.org/10.1016/j.advwatres.2013.01.001.

Phillips, T., Nerem, R.S., Fox-Kemper, B., Famiglietti, J.S., and Rajagopalan, B., (2012), The influence of ENSO on global terrestrial water storage using GRACE, GRL, 39, L16705, doi:10.1029/2012GL052495

Piper B. S., Plinston D.T., Sutcliffe, J. V., (1986), The water balance of Lake Victoria. J. Hydrological Sciences, 31(1), 25-37

Preisendorfer R., (1988). Principal component analysis in meteorology and oceanography. Elsevier: Amsterdam.

Reager J.T., and Famiglieti J.S. (2009), Global terrestrial water storage capacity and flood potential using GRACE. Geophysical Research Letters, 36, L23402,1-6

Rietbroek, R., Brunnabend, S.E., Dahle, C., Kusche, J., Flechtner, F., Schr\"{o}ter, J., and Timmermann, R. (2009), Changes in total ocean mass derived from GRACE, GPS, and ocean modeling with weekly resolution. Journal of Geophysical Research, 114, C11004, doi:10.1029/2009JC005449.

751 Saji N.H, Goswami, B.N., Vinayachandran, P.N., Yamagata, T.,1999: A dipole mode in the
752 tropical Indian Ocean. Nature 401:360–363
753 Stager J.C., Ruzmaikin A., Conway D., Verburg P., and Mason, P.J., (2007), Sunspots, El Nino,
754 and the levels of Lake Victoria, East Africa. Journal of Geophysical Research, VOL. 112,
755 D15106, doi:10.1029/2006JD008362
756 Swenson, S., and J. Wahr (2009), Monitoring the water balance of Lake Victoria, East Africa,
757 from space, Journal of Hydrology, 370, 163-176.
758 Tapley, B., Bettadpur, S., Ries, J., Thompson, P., and Watkins, M. (2004), GRACE
759 measurements of mass variability in the Earth system. Science,305,503-
760 505.http://dx.doi.org/10.1126/science.1099192
761 Thomas, A.C.; Reager, J.T.; Famiglietti, J.S.; Rodell, M. A (2014), GRACE-based water storage
762 deficit approach for hydrological drought characterization. Geophys. Res. Lett., 41,
763 1537–1545.
764 Wahr, J., Molenaar, M., and Bryan, F. (1998), Time variability of the Earth's gravity field:
765 Hydrological and oceanic effects and their possible detection using GRACE. Journal of
766 Geophysical Research, 103 (B12), 30205-30229, doi:10.1029/98JB02844.
767 Wolter K., and Timlin, M.S., (2011), El Nino/Southern Oscillation behaviour since 1871 as
768 diagnosed in an extended multivariate ENSO index (MEI.ext). International J.
769 Climatology,31(7),1074-1087
770 Zhang, Z.; Chao, B.; Chen, J.; Wilson, C. (2015), Terrestrial water storage anomalies of Yangtze
771 River Basin droughts observed by GRACE and connections with ENSO. Glob. Planet.
772 Chang., 126, 35–45.
773